

Fermionic states in pure 4D deconstruction

P. Q. Hung* and Ngoc-Khanh Tran†

Department of Physics, University of Virginia

382 McCormick Road, Charlottesville, Virginia 22904-4714, USA

(Dated: February 7, 2008)

Abstract

We study the structure of fermionic mass eigenstates in a pure four-dimensional deconstruction approach. Unlike the case with the usual higher dimensional deconstruction (or latticized extra dimension), here the doubling of fermionic degrees of freedom is physical, thus there is no need to invoke Wilson terms to eliminate them. The fermionic structure is shaped by two key factors, namely the boundary conditions on fermions and the ratio of two breaking scales involved. The singular value decomposition of linear algebra is employed to shed light into the phenomenologically crucial role of chiral boundary conditions. In this approach, we can explain the “localization” or “delocalization” nature of fermionic zero mode in flavor space and obtain analytically all higher modes. The application of boundary conditions on fermions to the implementation of CKM quark mixing is also found.

PACS numbers: 11.25.Mj, 12.15.Ff

*pqh@virginia.edu

†nt6b@virginia.edu

I. INTRODUCTION

In the past few years, a great amount of renewed interest has been placed in the theories with extra spatial dimensions. Intrinsically, models in these spaces are non-renormalizable, thus extra dimensional theory can be seen generally as an effective one, being valid only below some cut-off scale. The important issue of cut-off independence or dependence in such models, though could be argued in specific contexts, remains rather obscured. With the advent of the dimensional deconstruction (DD) concept [1, 2], there exists the possibility to construct extra dimensional (ED) scenarios at lower energy scale effectively from a renormalizable four-dimensional (4D) theory. The chiral nature of fermions at low energy as dictated by the standard model (SM) then requires the imposition of some type of chiral boundary conditions (CBC) on the fermions. The simplest CBC mimics the Dirichlet and Neumann boundary conditions used in the orbifold compactification of extra dimension (see e.g. [2]). In this work, making use of the singular value decomposition of linear algebra, we systematically identify and analyze the role of general classes of CBCs on the fermion mass-eigenstates after the deconstruction. It turns out in particular that the chiral zero-mode wave function possesses a non-trivial, localized or delocalized, distribution in the flavor space [3, 4].

The pattern of localization is found to depend exclusively on two factors. The first of them is the ratio of the two underlying breaking scales present in the general deconstruction scenario, namely the link field vacuum expectation value (VEV) and the fermion bare mass (which can also be seen dynamically as the VEV of a gauge-singlet scalar field). The other factor is the chiral boundary condition being employed.

To study the effect coming solely from the ratio of these VEVs on the localization, we first present an analytical derivation of fermion zero-mode wave function under the Dirichlet-Neumann CBC. In the flavor space, the link field VEV sets the “dimension” where fermions of all modes can live on, while the fermion bare mass sets the size of the “domain wall” wherein zero-modes are confined. The relative magnitude of these two scales then obviously has a crucial role in shaping the zero-mode localization. And for an appropriate choice of this ratio, the whole phenomenological applicability of fat-brane models is carried over to the dimensional deconstruction scenario due the similar localization behavior.

To see the fermion wave function’s dependence on the boundary conditions, we next

work with more general CBCs *a priori*. Here, the singular value decomposition (SVD) theorem proves to be a powerful tool in the systematic identification of CBC, with which the spectrum and wave functions of all modes can be exactly solved. In this sense, selecting boundary conditions also means modeling the outcome of the Kaluza-Klein (KK) spectrum. Furthermore, many related quantities, those are important in model building such as phase and wave function overlaps, can now be encoded concisely in the boundary conditions.

In the other perspective, it may be also tempting to geometrically embed the deconstruction group into a latticized extra dimension as has been done in [5, 6]. However, the well-known fermion flavor doubling problem in lattice models, or else the need of a faithful lattice representation of the continuum, requires some remedy such as the incorporation of Wilson terms into the Lagrangian. These terms however eliminate half of fermionic chiral degrees of freedom (see Appendix). It is for this reason that, in the literature, as far as the fermion sector is concerned, one usually starts with Weyl rather than Dirac spinors [2, 3, 4]. In this paper, motivated by the ability of dimensional deconstruction in providing the UV completion for ED models, we perform the deconstruction purely within the 4D framework (4D deconstruction), and will not build an actual latticized extra dimension to host the deconstruction product group [20]. This is equivalent to beginning with a set of Dirac spinors. It is shown that as long as the zero modes are concerned, the 4D deconstruction is not more complicated than the latticized ED model. Along this line of reasoning, it is worthwhile to note that in a 4D deconstruction context, fermions do not actually live in any exotic orbifold, and the concept of “boundary condition” mentioned above in reality can be perceived rather as a defect in some deconstruction group representation. That is why fermions of different flavors do not necessarily obey the same boundary conditions. And this fact can be used to model the quark families hierarchical mixings observed in standard model.

This work is structured as follows. In Section II we derive and analyze the localization patterns of zero mode fermion after the 4D deconstruction. The chiral nature of zero mode is also visualized in the analog coupled oscillator system. We recall the SVD theorem in Section IIIA and employ it to clarify the crucial role of CBC in the structuring of fermion mass eigenbasis in Section IIIB. Then we illustrate how complex CKM mixings and mass hierarchy of SM quarks could arrive from the appropriate selection of boundary condition in Section IIIC. We summarize the main results in Section IV. Finally, for the purpose of comparison, in the Appendix we recapitulate the essence of latticized ED scenario.

II. LOCALIZATION OF CHIRAL ZERO MODES IN FLAVOR SPACE

In the general dimensional deconstruction approach, fermions associated with different gauge groups are coupled to one another via scalar link fields through Yukawa interaction terms. By giving appropriate vacuum expectation value (VEV) to these link fields one can completely restructure the fermion mass spectrum and keep only its lightest modes to be the phenomenologically relevant ones at low energy. Such zero mode exposes some very interesting “localization” behavior in the group index space (also referred to as flavor space throughout), parallel to that of the split fermion scenario in extra dimension. Thus the pure 4D deconstruction mechanism can have vast applicabilities to phenomenology although no actual extra dimensions have been invoked.

A. Localization formation

The general setup of dimensional deconstruction contains a gauge group product $\prod_{n=1}^N G_n$ and N fermionic flavors ψ_n transforming fundamentally under the corresponding group G_n in the usual 4D space time. There are also $N - 1$ scalars $\phi_{n,n+1}$ living in the fundamental and anti-fundamental representation of G_n and G_{n+1} respectively. Hence each scalar couples to two “neighboring” groups and can be also referred to as a link field. For simplicity, we also assume the universal fermion-scalar-fermion couplings, which can be realized by imposing a permutation symmetry concerning the group index n . The gauge-invariant Lagrangian describing this “open moose” set-up reads as follows

$$\mathcal{L} = \sum_{n=1}^N \bar{\psi}_n i \not{D}_n \psi_n + \sum_{n=1}^{N-1} \bar{\psi}_n \phi_{n,n+1} \psi_{n+1} - \phi_S \sum_{n=1}^N \bar{\psi}_n \psi_n \quad (1)$$

where ϕ_S denotes a gauge-singlet scalar and \not{D}_n the covariant derivative. In respect to the above permutation symmetry, the following spontaneous symmetry breakings

$$\phi_S \rightarrow \langle \phi_S \rangle = M; \quad \phi_{n,n+1} \rightarrow \langle \phi_{n,n+1} \rangle = V \quad (\forall n) \quad (2)$$

give rise to a fermion mass structure. The gauge singlet vacuum expectation value M is also referred to as fermion bare mass hereafter. In the chiral basis

$$\{\psi_{L,R}^N\} \equiv \{\psi_{1L,R}, \dots, \psi_{NL,R}\}^T; \quad \{\bar{\psi}_{L,R}^N\} \equiv \{\bar{\psi}_{1L,R}, \dots, \bar{\psi}_{NL,R}\} \quad (3)$$

the mass term can be written as

$$\{\bar{\psi}_L^N\} [\mathcal{M}] \{\psi_R^N\} + \{\bar{\psi}_R^N\} [\mathcal{M}] \{\psi_L^N\} \quad (4)$$

with $[\mathcal{M}]$ being the $N \times N$ -dimension mass matrix

$$[\mathcal{M}]_{N \times N} = [\mathcal{M}]_{N \times N}^\dagger = \begin{pmatrix} M & -V & 0 \\ -V^* & M & -V \\ 0 & -V^* & M \\ & & \ddots \\ & & M & -V & 0 \\ & & -V^* & M & -V \\ & & 0 & -V^* & M \end{pmatrix} \quad (5)$$

Each link field transforms non-trivially under two groups and V assumes complex value in general [21]. In contrast, the gauge singlet vacuum expectation value M is always real as required by the hermiticity of the Lagrangian (1). It is obvious from Eq. (5) that this setup has all chiral fermion pairs degenerate in mass and thus describes a vector-like model. As in theories with EDs, in order to have a chiral model at low energy limit we need some chiral boundary conditions (CBC). In the context of dimensional deconstruction, these “CBCs” can be realized by adopting the following gauge-invariant asymmetric choice of fermion content in the chiral representation space [22]

$$\psi_{1R} = \psi_{NR} = 0; \quad \phi_{k-1,k} \psi_{k,L} = V \psi_{k-1,L} \quad (6)$$

In the truly extra dimensional set-up, the boundary conditions being asymmetric with respect to fermionic chiral components (i.e. chiral boundary conditions) are shown to be compatible with the variational principle [18] in e.g. Higgsless models [19]. In 4D deconstruction, the CBCs (6) literally are the “defects” in fermion representation at some particular sites. At least in the large N (i.e. continuum) limit, these CBCs too might follow from the application of variational principle on some appropriately constructed action. This approach to the 4D deconstruction CBCs is currently under our investigation.

The first “boundary condition” of (6) is simply the statement that ψ_{1L} and ψ_{NL} do not have matching right-handed counterparts. Notice also that the above boundary conditions break our permutation symmetry, a feature which is very analogous to the breaking of

translational symmetry in compact extra dimensions by orbifold boundary conditions. When the link fields assume VEV $\langle \phi \rangle = V$ and $k = 2$ (or N), Eq. (6) mimics the Dirichlet and Neumann boundary conditions [2]. However, in pure 4D deconstruction, there is no latticized ED to host the group chain. That is why there is no need to identify k to the “end-points” $k = 2$ (or N). Rather one can choose k to be any integer $\in [2, N]$. We can also write (6) in a systematic matrix notation

$$\begin{pmatrix} \psi_{1L} \\ \vdots \\ \psi_{NL} \end{pmatrix} = \{\psi_L^N\} = [\mathcal{B}_L]_{N \times (N-1)} \{\psi_L^{N-1}\} = \begin{pmatrix} 1 & & & \\ & \ddots & & \\ & & 1 & \\ & & & 1 \end{pmatrix} \begin{pmatrix} \psi_{1L} \\ \vdots \\ \psi_{k-1L} \\ \psi_{k+1L} \\ \vdots \\ \psi_{NL} \end{pmatrix}; \quad (7)$$

$$\begin{pmatrix} \psi_{1R} \\ \vdots \\ \psi_{NR} \end{pmatrix} = \{\psi_R^N\} = [\mathcal{B}_R]_{N \times (N-2)} \{\psi_R^{N-2}\} = \begin{pmatrix} 0 & 0 \\ 1 & & \\ & \ddots & \\ & & 1 \\ 0 & 0 \end{pmatrix} \begin{pmatrix} \psi_{2R} \\ \vdots \\ \psi_{N-1R} \end{pmatrix} \quad (8)$$

where $\{\psi_L^{N-1}\}$ and $\{\psi_R^{N-2}\}$ as defined in (7), (8) denote truly independent $N - 1$ left-handed and $N - 2$ right-handed fermionic degrees of freedom. Non-square matrices $[\mathcal{B}_L]$ and $[\mathcal{B}_R]$ precisely encode the chiral boundary conditions (6). These CBCs aim to break the L-R symmetry in the mass term (4), which now becomes

$$\{\bar{\psi}_L^{N-1}\} [\mathcal{M}_{LR}] \{\psi_R^{N-2}\} + \{\bar{\psi}_R^{N-2}\} [\mathcal{M}_{RL}] \{\psi_L^{N-1}\} \quad (9)$$

with chiral mass matrices

$$[\mathcal{M}_{LR}]_{(N-1) \times (N-2)} \equiv [\mathcal{B}_L]^\dagger [\mathcal{M}] [\mathcal{B}_R]; \quad [\mathcal{M}_{RL}]_{(N-2) \times (N-1)} \equiv [\mathcal{B}_R]^\dagger [\mathcal{M}] [\mathcal{B}_L] \quad (10)$$

By coupling the chiral Dirac equations

$$i \not{\partial} \{\psi_L^{N-1}\} - [\mathcal{M}_{LR}] \{\psi_R^{N-2}\} = 0; \quad i \not{\partial} \{\psi_R^{N-2}\} - [\mathcal{M}_{RL}] \{\psi_L^{N-1}\} = 0 \quad (11)$$

we see that the squared-mass matrix is $[\mathcal{M}_L^2]_{(N-1) \times (N-1)} \equiv [\mathcal{M}_{LR}] [\mathcal{M}_{RL}]$ for the left-handed components $\{\psi_L\}$ and $[\mathcal{M}_R^2]_{(N-2) \times (N-2)} \equiv [\mathcal{M}_{RL}] [\mathcal{M}_{LR}]$ for the right-handed $\{\psi_R\}$. In

Section III we will show that under any CBCs of the type (6), $[\mathcal{M}_L^2]$ always possesses zero eigenvalue, assuring the identification of its corresponding eigenstate with SM left-handed fermions. For now we just present the analytical derivation of this chiral massless eigenstate for any values of M and V .

First we note that because $[\mathcal{M}_{LR}]$ has dimension $(N-1) \times (N-2)$, its left inverse matrix $[\mathcal{M}_{LR}^{-1}]$ exists (i.e. $[\mathcal{M}_{LR}^{-1}][\mathcal{M}_{LR}] = \mathbf{1}$). Therefore the solution of zero eigen-problem of $[\mathcal{M}_L^2]$ is identical to that of $[\mathcal{M}_{RL}]$, i.e.

$$[\mathcal{M}_L^2]\{x_n^{N-1}\} = 0 \Leftrightarrow [\mathcal{M}_{RL}]\{x_n^{N-1}\} = 0 \quad (12)$$

where we have $N-1$ variables $\{x_n^{N-1}\} \equiv \{x_1, \dots, x_{k-1}, x_{k+1}, \dots, x_N\}^T$ in the notation of (7). Using the definition (10) of $[\mathcal{M}_{RL}]$, we can write (12) explicitly as

$$\rho^* x_{n-1} - x_n + \rho x_{n+1} = 0 \quad (n = 1, \dots, N) \quad (13)$$

with the newly introduced variable x_k being defined as $x_k \equiv x_{k-1}$ and

$$\rho \equiv \frac{V}{M} \equiv \frac{|V|e^{i\theta}}{M} \quad (14)$$

Since all link fields have been uniformly broken, the coefficients of (13) are all independent of index n . This in turn suggests a solution of the form $x_n = a \exp(bn)$. We obtain

$$x_n = \begin{cases} \mathcal{C} e^{-in\theta} [\sinh(k-n)\alpha - e^{i\theta} \sinh(k-1-n)\alpha] & \text{if } |\rho| < 1/2 \ (\cosh\alpha \equiv 1/2|\rho|) \\ 1/\sqrt{N-1} & \text{if } |\rho| = 1/2 \\ \mathcal{C} e^{-in\theta} [\sin(k-n)\alpha - e^{i\theta} \sin(k-1-n)\alpha] & \text{if } |\rho| > 1/2 \ (\cos\alpha \equiv 1/2|\rho|) \end{cases} \quad (15)$$

with the normalization factor \mathcal{C} satisfying

$$\sum_{n \neq k}^N |x_n|^2 = 1 \quad (16)$$

Physically, $\{x_n\}$ is interpreted as the weight of the zero mass eigenstate $\tilde{\psi}_0$ distributed in the flavor space $\{\psi_L\}$

$$\tilde{\psi}_0 = \{x_n^{N-1}\}^\dagger \{\psi_L^{N-1}\} = \sum_{n \neq k}^N x_n^* \psi_{nL} \quad (17)$$

Because of (16) and (17), $\{x_n\}$ can be referred to as “wave function” of fermion zero mode in the group index space. The explicit solution (15) reveals some very interesting properties of the massless eigenstate. First, this state is genuinely complex as long as V is. Second,

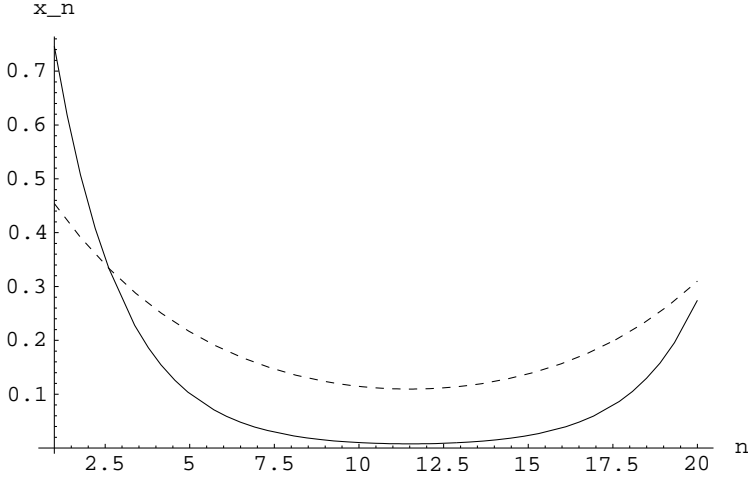


FIG. 1: Normalized wave function profile (18) with $k=12$ in flavor space. $\rho = 0.44$ (or $\alpha = 0.52$) for continuous line and $\rho = 0.49$ (or $\alpha = 0.20$) for dashed line. $N=20$ in both cases. The wave function with smaller ρ is more localized.

(15) may have a localized or oscillatory behavior in the group index space depending on the value of underlying parameters (see Section IIB). Both of these properties have important applications among others to the characterization of CP violation and fermion mass hierarchy in the Standard Model. We now will explore quantitatively the behavior of this localization mechanism in the dimensional deconstruction scenario.

B. Pattern of localization

The chiral zero mode wave function (15) has a clear dependence on the ratio $\frac{V}{M}$ of link field and gauge-singlet scalar VEVs. For a pure view on the nature of localization, we can just assume for the moment that V is real (i.e. $\theta = 0$ in (14)). In this case (15) looks particularly simple

$$x_n = \begin{cases} \mathcal{C} \cosh(k - n - 1/2)\alpha & \text{if } \rho < 1/2 \ (\cosh \alpha \equiv 1/2\rho) \\ 1/\sqrt{N-1} & \text{if } \rho = 1/2 \\ \mathcal{C} \cos(k - n - 1/2)\alpha & \text{if } \rho > 1/2 \ (\cos \alpha \equiv 1/2\rho) \end{cases} \quad (18)$$

For $\rho \equiv V/M < 1/2$, zero mode wave function has a localized profile described by a cosh function (Fig. 1). This can be explained both physically and mathematically as follows. As $\rho < 1/2$, the linkage symmetry breaking induced mass (proportional to V) of fermions

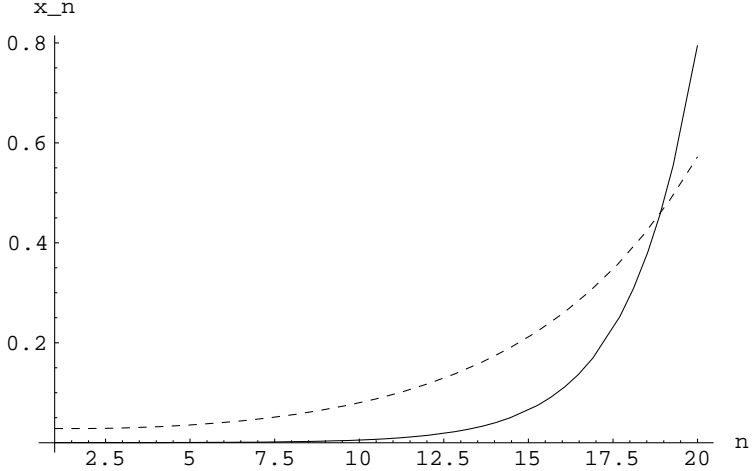


FIG. 2: Normalized wave function profile (18) with $k=2$ in flavor space. $\rho = 0.44$ (or $\alpha = 0.52$) for continuous line and $\rho = 0.49$ (or $\alpha = 0.20$) for dashed line. $N=20$ in both cases. The wave function with smaller ρ is more localized.

is essentially smaller than their bare mass M . In an intuitive approach inspired by the ED perspective, $L_V \equiv \frac{1}{V}$ sets the size of the “extra dimension” (see Eq. (34) below) and $L_M \equiv \frac{1}{M}$ sets the size of the “domain wall”, to which chiral fermion is trapped in the discretized version of Jackiw-Rebbi localization mechanism [8, 9]. [23] Clearly, localization makes sense only when $L_M \ll L_V$ (i.e. $\rho \ll 1$). In a more quantitative approach, as $V < \frac{M}{2}$, the gauge eigenstates $\{\psi_{L,R}^n\}$ well resemble the mass eigenstates $\{\tilde{\psi}_{L,R}^n\}$. And when $k \neq 2$ (and N), the CBC (6) on right-handed fields $\psi_{1R} = \psi_{NR} = 0$ implies that their opposite (unpaired) chiral partners ψ_{1L} and ψ_{NL} remain approximately massless chiral states. That is why in Fig. 1 we see that the exact chiral zero mode indeed is dominated by ψ_{1L} and ψ_{NL} . In the special cases where $k = 2$ (or N), the CBC (6) on left-handed fields eliminates ψ_{1L} (or ψ_{NL}) from the set of truly independent fermionic degrees of freedom. Then the exact chiral zero mode is dominated only by ψ_{NL} (or ψ_{1L}), i.e. localization is around “fixed-point” $n=N$ in Fig. 2 (or $n=1$ in Fig. 3).

In all cases, the localized wave functions are exponentially suppressed into the middle values of n . Let us also remind ourselves that $k = 2$ (or N) corresponds to the familiar Dirichlet-Neumann boundary conditions in literature [2].

Mathematically, from Eq. (13), $\rho < 1/2$ requires that $x_{n-1} + x_{n+1} > 2x_n$, i.e. wave function profile should be concave. Together with the boundary condition $x_k = x_{k-1}$, this

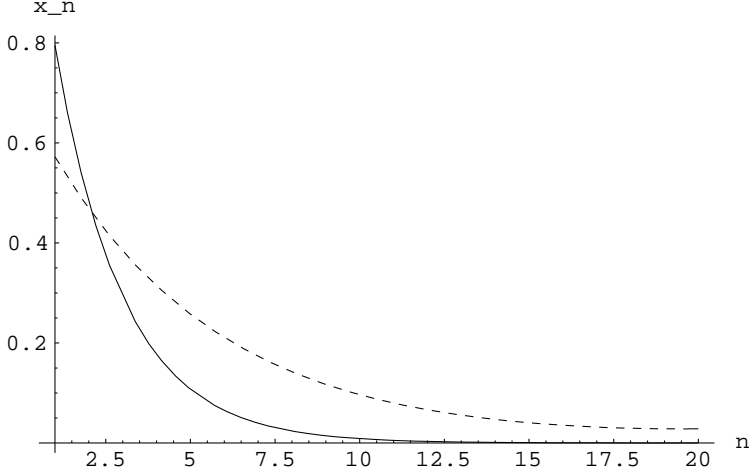


FIG. 3: Normalized wave function profile (18) with $k=20$ in flavor space. $\rho = 0.44$ (or $\alpha = 0.52$) for continuous line and $\rho = 0.49$ (or $\alpha = 0.20$) for dashed line. $N=20$ in both cases. The wave function with smaller ρ is more localized.

implies $x_1 > \dots > x_{k-1} = x_k < \dots < x_N$, so that wave function is “pushed” away from site $n=k$. Finally, in practical application, one may want to localize the chiral zero mode around some arbitrary site $n = k$. This can be done very effectively by simply combining the two localization patterns presented above, i.e. by the imposition of the following boundary conditions

$$\psi_{1R} = \psi_{kR} = 0 \quad \phi_{1,2}\psi_{2L} = V\psi_{1L} \quad (19)$$

$$\psi_{kR} = \psi_{NR} = 0 \quad \phi_{N-1,N}\psi_{NL} = V\psi_{N-1L} \quad (20)$$

In this case, (19) makes $x_1 \ll x_k$, while (20) makes $x_k \gg x_N$, so that the localization around $n = k$ is realized. Indeed, for these combined BCs, the detailed computation yields the following wave function distribution in the group index space (Fig. 4):

$$x_n = \begin{cases} \mathcal{C} \cosh [(N - k - 1/2)\alpha] \cosh [(n - 3/2)\alpha] & \text{for } 1 \leq n \leq k \\ \mathcal{C} \cosh [(N - n - 1/2)\alpha] \cosh [(k - 3/2)\alpha] & \text{for } k \leq n \leq N \end{cases} \quad (21)$$

where $\cosh \alpha \equiv 1/2\rho$ and \mathcal{C} is the normalization constant determined by $\sum_{n=2}^{N-1} |x_n|^2 = 1$. The overlap of two wave functions localized around $n = k_1$ and $n = k_2$ can be exactly computed from the analytical expression (21). In the leading order it is

$$\sum_{n=1}^N x_n^{(1)} x_n^{(2)} \sim e^{-|k_1\alpha_1 - k_2\alpha_2|} \quad (22)$$

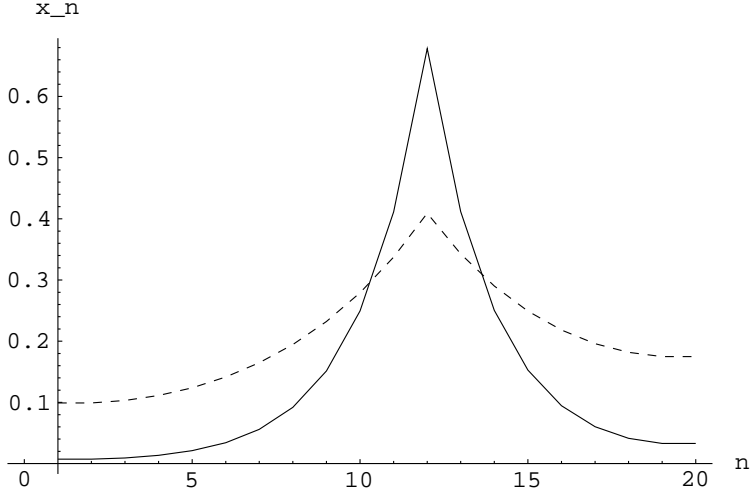


FIG. 4: Normalized wave function profile (21) with $k=12$ in flavor space. $\rho = 0.44$ (or $\alpha = 0.52$) for continuous line and $\rho = 0.49$ (or $\alpha = 0.20$) for dashed line. $N=20$ in both cases. The wave function with smaller ρ is more localized.

Evidently, the overlap is exponentially suppressed by the separation between localization centers. It also depends on the localization pattern of the underlying wave functions characterized by parameters α_1, α_2 . This property is a strong reminiscence of the spit fermion model in the extra dimension.

For $\rho \equiv V/M > 1/2$, the symmetry breaking effect prevails over the bare mass. Even with CBC (6), gauge eigenstates ψ_{1L} and ψ_{NL} no longer necessarily dominate the massless eigenstates. The massless mode oscillates like a trigonometric function (18) in the group index space. However, in this case the number of groups N also plays an important role. One can have a truly oscillatory wave function (Fig. 5) only if N is larger than the oscillation period ($\approx 2\pi/\alpha$). Else if $N < \pi/\alpha$, the CBC (6) produces a weakly (quasi) localized zero mode wave function around $n = k$ (Fig. 5).

The analysis of the case $\rho = 1/2$ can offer a physical insight on the single chirality nature of the massless mode and will be presented next.

C. Perfect delocalization

We first note that when $|\rho| = 1/2$, the system (13) has a solution only if $\theta = 0$ or 2π . This implies that for $|\rho| = 1/2$, CBC (6) is compatible only with real V . In this case the

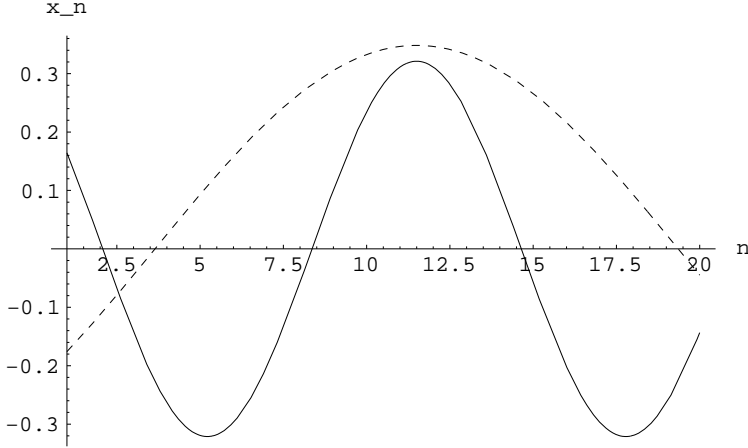


FIG. 5: Normalized wave function profile (18) with $k=12$ in flavor space. $\rho = 0.57$ (or $\alpha = 0.50$) for continuous line and $\rho = 0.51$ (or $\alpha = 0.20$) for dashed line. $N=20$ in both cases. The wave function with larger ρ exposes a truly oscillatory pattern.

zero mode is real and independent of index n , i.e. the wave function is flat (or perfect delocalization) in the group index space (15).

We leave a rigorous analysis of the chiral boundary conditions in deconstruction mechanism for Section III. For now, however, we are content with presenting a visualized physical picture on the chiral nature of zero modes by drawing the connection between dimensional deconstruction and the classical spring-ball chain system. The massless left and right-handed mode, if they exist, must be the solution of following equations (in the notation of Eq. (12))

$$[\mathcal{M}_L^2]\{x_n^{N-1}\} = 0; \quad [\mathcal{M}_R^2]\{y_n^{N-2}\} = 0 \quad (23)$$

where x and y respectively denote left and right-handed solution. The analysis below holds for any value of k in Eq. (6), but to keep the presentation simple, we choose to work with

$k = N$. In this case the chiral squared-mass matrices are

$$\frac{[\mathcal{M}_L^2]}{V^2} = \begin{pmatrix} 1 & -\rho^{-1} & 1 & 0 \\ -\rho^{-1} & 1 + \rho^{-2} & -2\rho^{-1} & 1 \\ 1 & -2\rho^{-1} & 2 + \rho^{-2} & -2\rho^{-1} \\ 0 & 1 & -2\rho^{-1} & 2 + \rho^{-2} \\ & & \ddots & \\ & & & -2\rho^{-1} & 2 + \rho^{-2} & -2\rho^{-1} & 1 \\ & & & 1 & -2\rho^{-1} & 2 + \rho^{-2} & 1 - 2\rho^{-1} \\ & & & 0 & 1 & 1 - 2\rho^{-1} & 2 - 2\rho^{-1} + \rho^{-2} \end{pmatrix} \quad (24)$$

$$\frac{[\mathcal{M}_R^2]}{V^2} = \begin{pmatrix} 2 + \rho^{-2} & -2\rho^{-1} & 1 & 0 \\ -2\rho^{-1} & 2 + \rho^{-2} & -2\rho^{-1} & 1 \\ 1 & -2\rho^{-1} & 2 + \rho^{-2} & -2\rho^{-1} \\ & & \ddots & \\ & & & -2\rho^{-1} & 2 + \rho^{-2} & -2\rho^{-1} & 1 \\ & & & 1 & -2\rho^{-1} & 2 + \rho^{-2} & 1 - 2\rho^{-1} \\ & & & 0 & 1 & 1 - 2\rho^{-1} & 2 - 2\rho^{-1} + \rho^{-2} \end{pmatrix} \quad (25)$$

In the analog spring-ball system, $[\mathcal{M}_{L,R}^2]$ represent the characteristic matrix of the system's oscillation. The mass eigenvalues and mass eigenstates correspond to the proper frequencies and the displacement amplitudes of the oscillation.

The fact that, for $\rho = 1/2$, the sum of all entries in any row of $[\mathcal{M}_L^2]$, and in any row except the first two of $[\mathcal{M}_R^2]$, vanishes allows us to identify the left sector with a free-end spring-ball system, and the right sector with an one-fixed-end system. Indeed, the characteristic matrix

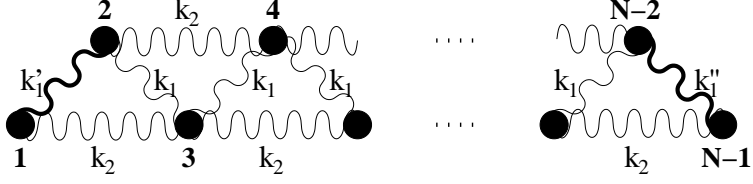


FIG. 6: Free-end and next-to-nearest-neighbor coupled oscillators' system.

describing the oscillation of free-end system depicted in Fig. 6 explicitly is

$$[\Omega_{free}] = \begin{pmatrix} k'_1 + k_2 & -k'_1 & -k_2 & 0 \\ -k'_1 & k'_1 + k_1 + k_2 & -k_1 & -k_2 \\ -k_2 & -k_1 & 2k_2 + 2k_1 & -k_1 \\ 0 & -k_2 & -k_1 & 2k_2 + 2k_1 \\ & & & \ddots \\ & & & -k_1 & 2k_2 + 2k_1 & -k_1 & -k_2 \\ & & & -k_2 & -k_1 & k_2 + k_1 + k''_1 & -k''_1 \\ & & & 0 & -k_2 & -k''_1 & k_2 + k''_1 \end{pmatrix} \quad (26)$$

and the matrix describing the oscillation of one-fixed-end system depicted in Fig. 7

$$[\Omega_{fixed}] = \begin{pmatrix} k''_1 + k_1 + k_2 & -k_1 & -k_2 & 0 \\ -k_1 & 2k_2 + 2k_1 & -k_1 & -k_2 \\ -k_2 & -k_1 & 2k_1 + 2k_2 & -k_1 \\ & & & \ddots \\ & & & -k_1 & 2k_2 + 2k_1 & -k_1 & -k_2 \\ & & & -k_2 & -k_1 & k_2 + k_1 + k''_1 & -k''_1 \\ & & & 0 & -k_2 & -k''_1 & k_2 + k''_1 \end{pmatrix} \quad (27)$$

When $\rho = 1/2$, we can evidently identify (24) with (26), and (25) with (27) by specifying the springs' constants as follows

$$k_1 = \frac{2}{\rho} = 4; \quad k_2 = -1; \quad k'_1 = \frac{1}{\rho} = 2; \quad k''_1 = -1 + \frac{2}{\rho} = 3 \quad (28)$$

Next we note that, by giving an uniform displacement to the balls, the free-end system moves from one equilibrium position to another. And since the equilibrium can be seen as

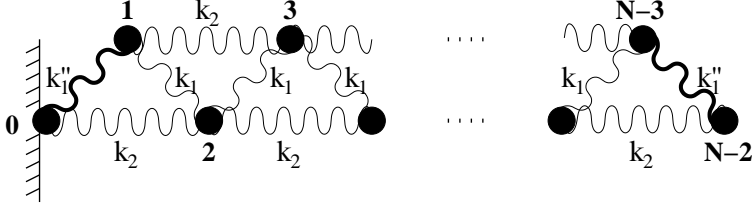


FIG. 7: One-fixed-end and next-to-nearest-neighbor coupled oscillators' system.

the oscillation with null frequency, the left squared-mass matrix $[\mathcal{M}_L^2]$ certainly possesses a zero mass eigenstate and a corresponding uniform eigenstate. That is why we have a flat left-handed zero mode wave function. In contrast, the fixed-end system does not have a translational symmetry, thus $[\mathcal{M}_R^2]$ generally does not have a zero eigenvalue, i.e. all right-handed fields are massive. For the gauge boson sector, and in the Higgsless scenario, the similar analog spring-ball systems have been used in [10] to illustrate the mass structure of neutral and charged boson towers.

For any other values of ρ , one can multiply each column of $[\mathcal{M}_L^2]$ by a factor so that the sum of all entries in any row of the new formed matrix vanishes. Such factors can always be found because the determinant of $[\mathcal{M}_L^2]$ is zero as shown in the next section. Then we can construct explicitly the new analog free-end classical oscillator system, which necessarily possesses a zero mode. However, in this general case the ultimate zero mode wave function is no longer flat, because its components are obtained by scaling back from a uniform profile with different factors. The determinant of $[\mathcal{M}_R^2]$ does not vanish thus it cannot be attributed to any free-end system, and the right-handed sector does not have a massless mode in general.

In 4D deconstruction, as explained in the appendix, due to the legitimate presence of all chiral degrees of freedom, the squared-mass matrices $[\mathcal{M}_L^2]$, $[\mathcal{M}_R^2]$ usually correspond to a next-to-nearest neighbor interaction of coupled oscillators. As a result, the mass spectrum and wave functions of massive modes in general cannot be found exactly, although their perturbative expansions can always be obtained. Fortunately, there exist methods to identify classes of CBC, whereby the 4D deconstruction can be brought down to nearest-neighbor interaction in the language of an analog classical system as we shall see next.

III. MODELING OF MASSIVE FERMIONIC STATES

In the previous section we have studied the fermion chiral zero mode resulting from the imposition of chiral boundary condition of the type (6). Intuitively, because of CBCs (6), there is one more left-handed independent component than the right-handed partners. The extra left-handed field cannot be put into a Dirac mass term, so it constitutes a chiral zero mode. We now perform a deeper analysis on the chiral nature of zero mode, using the linear algebra theorem of singular value decomposition (SVD). It turns out that, the theorem also leads to the specification of classes of boundary conditions, with which the entire mass eigenstate and eigenvalue system can be *exactly* solved.

A. Singular Value Decomposition

First we present the statement of SVD theorem. Let $[\mathcal{S}]$ be a complex matrix of dimension $m \times n$. Without the lost of generality we assume $m > n$. Then $[\mathcal{S}]$ can always be written in the SVD form: $[\mathcal{S}] = [\mathcal{U}][\Sigma][\mathcal{V}]^\dagger$, where $[\mathcal{U}]$ and $[\mathcal{V}]$ are unitary matrices of dimension $m \times m$ and $n \times n$ respectively, and $[\Sigma]$ is a $m \times n$ -dimension diagonal real matrix (i.e. $[\Sigma]_{p,q} \sim \delta_{p,q}$). The proof of this theorem can be found e.g. in [11].

The SVD theorem allows the chiral mass matrix $[\mathcal{M}_{LR}]_{(N-1) \times (N-2)}$ (10) to be decomposed as

$$[\mathcal{M}_{LR}] = [\mathcal{U}][\Sigma][\mathcal{V}]^\dagger = [\mathcal{U}] \begin{pmatrix} m_1 & & & \\ & \ddots & & \\ & & m_{N-2} & \\ & & & 0 \end{pmatrix} [\mathcal{V}]^\dagger \quad (29)$$

where $\{m_n\}$ is some set of real numbers. Since $[\mathcal{M}_{RL}] = [\mathcal{M}_{LR}]^\dagger$, we obtain immediately the squared-mass matrices defined below Eq. (11)

$$[\mathcal{M}_L^2] = [\mathcal{U}]([\Sigma][\Sigma]^T)[\mathcal{U}]^\dagger = [\mathcal{U}] \begin{pmatrix} m_1^2 & & & \\ & \ddots & & \\ & & m_{N-2}^2 & \\ & & & 0 \end{pmatrix} [\mathcal{U}]^\dagger \quad (30)$$

$$[\mathcal{M}_R^2] = [\mathcal{V}]([\Sigma]^T[\Sigma])[\mathcal{V}]^\dagger = [\mathcal{V}] \begin{pmatrix} m_1^2 & & \\ & \ddots & \\ & & m_{N-2}^2 \end{pmatrix} [\mathcal{V}]^\dagger \quad (31)$$

Because a unitary rotation leaves the eigenvalues of a matrix unchanged, we see clearly that there is a massless left-handed mode, and all massive modes come in pair of opposite chiralities. We also see that \mathcal{U} and \mathcal{V} actually diagonalizes \mathcal{M}_L^2 and \mathcal{M}_R^2 respectively.

B. The construction of fermion higher modes

The Dirichlet and Neumann boundary conditions (6) produce a simple, in part localized, chiral zero mode of fermion in the framework of 4D deconstruction. As in non-universal extra dimension (i.e. brane) models, one needs to quantitatively make sure that the contribution of higher Kaluza-Klein states to the precisely measured electroweak observables is sufficiently small. However, the higher mode structure following these CBCs cannot be exactly determined as mentioned earlier. We now attempt to specify other classes of CBC, which give rise to an exact and simple structure of fermion massive tower, apart from a chiral massless mode.

First, we begin our construction with the original mass matrix $[\mathcal{M}]$ (5), which truly characterizes the mixing of fermion flavors in a vector-like set-up, when no boundary conditions are imposed. Because it is hermitian, \mathcal{M} can be diagonalized by a unitary matrix $[\mathcal{U}_M]$

$$[\mathcal{M}] = [\mathcal{U}_M]^\dagger [\mathcal{M}_D] [\mathcal{U}_M] = [\mathcal{U}_M]^\dagger \begin{pmatrix} M_1 & & \\ & \ddots & \\ & & M_N \end{pmatrix} [\mathcal{U}_M] \quad (32)$$

Since $[\mathcal{M}]$ also describes the spring-ball system with only nearest-neighbor interaction, $[\mathcal{M}_D]$ and $[\mathcal{U}_M]$ can be worked out exactly. Indeed, the eigen-system equation associated with $[\mathcal{M}]$ (5) reads

$$-V^*U_{n-1,k}^M + MU_{n,k}^M - VU_{n+1,k}^M = M_k U_{n,k}^M \quad (n = 0, \dots, N+1) \quad (33)$$

where M_k and $\{U_{n,k}^M\}$ denote respectively the k -th eigenvalue and eigenstate in the notation of Eq. (32). To streamline the presentation we have also introduced extra components $U_{0,k}^M$ and $U_{N+1,k}^M$, which are identically zero: $U_{0,k}^M = U_{N+1,k}^M = 0$. The same method that solved

Eq. (13) now yields

$$M_k = M \left(1 - 2 \frac{|V|}{M} \cos \frac{k\pi}{N+1} \right) \quad (k = 1, \dots, N) \quad (34)$$

$$U_{n,k}^M = \sqrt{\frac{2}{N}} e^{-in\theta} \sin \frac{nk\pi}{N+1} \quad (n = 1, \dots, N) \quad (35)$$

Here, we in particular note that when $|\rho| = \frac{|V|}{M} > \frac{1}{2}$, there may be an accidental degeneration in the zero mode of the construction presented below (i.e. when $M_k = 0$ in Eq. (34)). This in turn would spoil the single chirality desired for the zero mode under construction. It is then natural to assume $|\rho| \leq \frac{1}{2}$ -an explicit bound on ρ that could not have been set by otherwise just looking at the localization pattern of the zero mode itself.

Next, from Eqs. (10), (29) and (32) we have the following equality

$$[\mathcal{U}] [\Sigma] [\mathcal{V}]^\dagger = [\mathcal{B}_L]^\dagger [\mathcal{U}_M]^\dagger [\mathcal{M}_D] [\mathcal{U}_M] [\mathcal{B}_R] \quad (36)$$

On the left-hand side, $[\Sigma]$ as defined in Eq. (29) contains all $N - 2$ eigen-masses $\{m_n\}_1^{N-2}$ of massive modes that we want to determine. On the right-hand side, $[\mathcal{M}_D]$ (32) contains N known eigen-masses (34) of the vector-like model. In a straightforward construction, we wish to identify $\{m_n\}_1^{N-2}$ with $N - 2$ eigenvalues of vector-like matrix $[\mathcal{M}]$, say $\{M_n\}_1^{N-2}$. This can be realized in many different ways. Just for the purpose of illustration, we present below a particular, not necessarily simplest, choice of SVD unitary matrices $[\mathcal{U}]$, $[\mathcal{V}]$ and the boundary conditions $[\mathcal{B}_L]$, $[\mathcal{B}_R]$ that fulfill this identification requirement.

$$[\mathcal{V}] = \mathbf{1}_{(N-2) \times (N-2)}; \quad [\mathcal{U}] = \begin{pmatrix} \mathbf{1}_{(N-3) \times (N-3)} & & \\ & \frac{1}{\sqrt{2}} & \frac{1}{\sqrt{2}} \\ & -\frac{1}{\sqrt{2}} & \frac{1}{\sqrt{2}} \end{pmatrix} \quad (37)$$

$$[\mathcal{B}_L]_{N \times (N-1)} = \begin{pmatrix} U_{1,1}^M & \dots & \dots & U_{1,N}^M \\ \vdots & \ddots & \dots & \vdots \\ U_{N-3,1}^M & \dots & \dots & U_{N-3,N}^M \\ U_{N-2,1}^M/\sqrt{2} & \dots & \dots & U_{N-2,N}^M/\sqrt{2} \\ -U_{N-2,1}^M/\sqrt{2} & \dots & \dots & -U_{N-2,N}^M/\sqrt{2} \end{pmatrix}^\dagger \quad (38)$$

$$[\mathcal{B}_R]_{N \times (N-2)} = \begin{pmatrix} U_{1,1}^M & \dots & \dots & U_{1,N}^M \\ \vdots & \ddots & \dots & \vdots \\ U_{N-3,1}^M & \dots & \dots & U_{N-3,N}^M \\ U_{N-2,1}^M & \dots & \dots & U_{N-2,N}^M \end{pmatrix}^\dagger \quad (39)$$

where $U_{k,q}^M$ is the element in the k -th row and q -th column of the matrix $[\mathcal{U}_M]$ (Eq. (35)) that diagonalizes the matrix \mathcal{M} (32). Because $[\mathcal{U}_M]$ is unitary, we can verify that Eq. (36) holds for the choice (37)-(39).

As a result of this particular construction, the spectrum of deconstructed fermions contains one left-handed zero mode and $N - 2$ higher vector-like modes of the masses identical to the eigenvalues M_k ($k = 1, \dots, N - 2$) (Eq. (34)) of the original vector-like mass matrix $[\mathcal{M}]$.

The combination of Eqs. (7), (8), (35), (38) and (39) gives the explicit CBC needed in the realization of this construction [24]. Generally, from Eqs. (30), (31) and the discussion below Eq. (11) we see that the corresponding wave functions of left and right-handed eigen-modes are just the column vectors of SVD unitary matrices \mathcal{U} and \mathcal{V} respectively. Specifically for the choice (37)-(39), most of states in mass eigenbasis are identical to those in flavor eigenbasis as indicated by the explicit expression (37). The only two exceptions are the massless and $(N - 2)$ -th massive left-handed states, which are written in flavor space as (see Eqs. (17), (37))

$$\tilde{\psi}_{0L} = \frac{1}{\sqrt{2}}(\psi_{N-2L} + \psi_{N-1L}); \quad \tilde{\psi}_{N-2L} = \frac{1}{\sqrt{2}}(\psi_{N-2L} - \psi_{N-1L}) \quad (40)$$

As before, $\tilde{\psi}$ and ψ respectively denote mass and flavor eigenstates.

The mass eigenstates (40) may look rather simple, but we can easily and systematically make all mass eigenstates more involved into the flavor space as follows. First we introduce the new boundary conditions $[\mathcal{B}_L] \rightarrow [\mathcal{B}'_L] \equiv [\mathcal{B}_L][\mathcal{U}_L]$; $[\mathcal{B}_R] \rightarrow [\mathcal{B}'_R] \equiv [\mathcal{B}_R][\mathcal{U}_R]$ where $[\mathcal{U}_L]$ and $[\mathcal{U}_R]$ are some unitary matrices of dimension $(N - 1) \times (N - 1)$ and $(N - 2) \times (N - 2)$ respectively. The chiral squared-mass matrices accordingly transform as (see Eq. (10)) $[\mathcal{M}_L^2] \rightarrow [\mathcal{M}'_L^2] = [\mathcal{U}_L]^\dagger [\mathcal{M}_L^2] [\mathcal{U}_L]$ and $[\mathcal{M}_R^2] \rightarrow [\mathcal{M}'_R^2] = [\mathcal{U}_R]^\dagger [\mathcal{M}_R^2] [\mathcal{U}_R]$. Obviously, this unitary transformation does not alter the mass structure of fermions. New and old CBC then can be referred to as being in the same class of *unitarily equivalent* boundary conditions. In contrast, this change of boundary condition deeply affects the distribution of mass eigenstates in flavor space. For the old boundary condition it is $\{\tilde{\psi}_L\} = [\mathcal{U}]^\dagger \{\psi_L\}$ and $\{\tilde{\psi}_R\} = [\mathcal{V}]^\dagger \{\psi_R\}$ respectively for left and right sectors. For the new boundary condition, it becomes $\{\tilde{\psi}'_L\} = [\mathcal{U}]^\dagger [\mathcal{U}_L] \{\psi_L\}$ and $\{\tilde{\psi}'_R\} = [\mathcal{V}]^\dagger [\mathcal{U}_R] \{\psi_R\}$. Making appropriate choice of matrices $[\mathcal{U}_L] \in U(N - 1)$ and $[\mathcal{U}_R] \in U(N - 2)$, we can flexibly modify the appearance of all mass eigenstates in the flavor space, but without changing the mass eigenvalues themselves.

Because the 4D propagation of massive particles is proportional to the inverse of their squared mass, the suppression of exotic fermion higher mode contribution primarily depends on their masses. Hence the construction above can have relevant applications in model building. Through the boundary conditions, we can alter the shape of chiral zero mode while still keeping under a permanent suppression all the effects induced by higher modes of a prefixed mass spectrum. In the next section we will illustrate this point in the building of quark mass hierarchy.

C. Application: Complex CKM mixing via chiral boundary condition

In this section we construct the mass hierarchy of SM quarks by having different “overlaps” of zero-mode fermion in flavor space. It would be interesting to apply the results derived in Section II to the construction of a model of fermion masses, using the idea of “localization” in group index space. This has been carried out in Ref. [12] (see also [4]). In the current work, we adopt a different approach to emphasize the effect of deconstruction boundary conditions. Here all quarks involved come from a single class of unitarily equivalent boundary conditions, thus they have the same mass spectrum as in the universal ED scenario. The distinct wave functions, and hence their overlaps as well as the CP violating phase, all are encoded concisely in the boundary conditions. Another mechanism to generate fermion mass hierarchy using arbitrary link field transformations has been proposed in [13].

We first identify the deconstruction product group as $\prod_{n=1}^N G_n \equiv \prod_{n=1}^N [SU(2) \times U(1)]_n$. To each member $[SU(2) \times U(1)]_n$ of the group chain we associate a $SU(2)_n$ -doublet scalar Higgs H_n , three $SU(2)_n$ -doublets $Q_n^{(i)}$ and six $SU(2)_n$ -singlets $U_n^{(i)}, D_n^{(i)}$ of spin $\frac{1}{2}$, just like in the standard model (with family index $i = 1, 2, 3$). The deconstruction interaction among $Q_n^{(i)}$ themselves (or $U_n^{(i)}$, or $D_n^{(i)}$) and the appropriate CBCs give rise to a zero mode of desired chirality as required by SM. The Yukawa interaction with Higgs fields next generates the mass for these zero modes. In this scenario, it is tempting to place the source of mass hierarchy solely in the difference of zero-mode distribution in DD group index space, so we assume the universal Yukawa couplings within Up and Down sectors. From the gauge-invariant Yukawa terms

$$\kappa_U \sum_{n=1}^N \bar{Q}_n^{(i)} i\sigma_2 H_n^* U_n^{(j)} + \kappa_D \sum_{n=1}^N \bar{Q}_n^{(i)} H_n D_n^{(j)} + H.c. \quad (41)$$

and given a uniform VEV of all Higgses $\langle H_n \rangle = h$ in accordance with the permutation symmetry, we can extract the mass terms for zero modes

$$h\kappa_U \sum_{i,j=1}^3 \bar{Q}_0^{(i)} M_{ij}^U \tilde{U}_0^{(j)} + h\kappa_D \sum_{i,k=1}^3 \bar{Q}_0^{(i)} M_{ik}^D \tilde{D}_0^{(k)} \quad (42)$$

where

$$M_{ij}^U = \sum_{n=1}^{N-1} [\mathcal{U}_Q^{(i)}]_{nN-1}^* [\mathcal{U}_U^{(j)}]_{nN-1} = [\mathcal{U}_Q^{(i)\dagger} \mathcal{U}_U^{(j)}]_{N-1, N-1} \quad (43)$$

$$M_{ij}^D = \sum_{n=1}^{N-1} [\mathcal{U}_Q^{(i)}]_{nN-1}^* [\mathcal{U}_D^{(j)}]_{nN-1} = [\mathcal{U}_Q^{(i)\dagger} \mathcal{U}_D^{(j)}]_{N-1, N-1} \quad (44)$$

To arrive to these expressions for zero-mode mass matrices we have used the facts that $\mathcal{U}_Q^{(i)}$ diagonalizes the squared-mass matrix $[\mathcal{M}_{QL}^{2(i)}]$ (30), and that in the convention of (30), the zero eigenvalue is placed in the bottom right entry of a matrix of dimension $(N-1) \times (N-1)$. Similar notations for U and D fields have been also assumed.

As discussed in the last part of previous section, the zero-mode coefficients $[\mathcal{U}_{Q,U,D}^{(j)}]_{nN-1}$ can be easily regulated by modifying the boundary condition. We consider here a simple three-site gauge model $[SU(2) \times U(1)]^3$ (i.e. $N = 3$). The CBCs on all quarks in general are different, we however assume that they belong to a single unitarily equivalent class (see Section IIIB), which also includes the “reference” Dirichlet-Neumann CBC (6). In this case, when $\rho = 1/2$, the actual wave function of any zero-mode quark is recovered from the “reference” zero mode by a rotation [25]

$$\left\{ [\mathcal{U}_Q^{(i)}]_{n,N-1} \right\}_{n=1}^{N-1} = \exp \left(i \vec{\alpha}_Q^{(i)} \frac{\vec{\tau}}{2} \right) \left\{ \frac{1}{\sqrt{N-1}} \right\}_1^{N-1} \quad (45)$$

where $N = 3$ and τ 's denote Pauli matrices. The uniform $(N-1)$ -dimensional vector $\left\{ \frac{1}{\sqrt{N-1}} \right\}_1^{N-1}$ represents the “reference” flat zero mode (15) obtained in Section II for the Dirichlet-Neumann CBC [26]. The generic $SU(N-1)$ matrix characterized by $\vec{\alpha} = (\alpha_x, \alpha_y, \alpha_z)$ implements the deviation of the actual CBC from that of the reference configuration for the case $N = 3$. The characterization similar to (45) can also be given for U and D fields. Plugging (45) into (43), (44) we obtain the mass matrix elements

$$M_{ij}^U = \frac{1}{N-1} \sum_{n,k=1}^3 \left[\exp \left(i(-\vec{\alpha}_Q^{(i)} + \vec{\alpha}_U^{(j)}) \frac{\vec{\tau}}{2} \right) \right]_{n,k} \quad (46)$$

$$M_{ij}^D = \frac{1}{N-1} \sum_{n,k=1}^3 \left[\exp \left(i(-\vec{\alpha}_Q^{(i)} + \vec{\alpha}_D^{(j)}) \frac{\vec{\tau}}{2} \right) \right]_{n,k} \quad (47)$$

Using the equality $\exp(i\vec{\alpha}\vec{\tau}) = \cos(|\alpha|/2) + i\frac{\vec{\alpha}}{|\alpha|}\vec{\tau} \sin(|\alpha|/2)$ we can write (46), (47) more explicitly as

$$M_{ij}^U = \cos \frac{|-\alpha_Q^{(i)} + \alpha_U^{(j)}|}{2} + i \frac{-\alpha_{Qx}^{(i)} + \alpha_{Ux}^{(j)}}{|-\alpha_Q^{(i)} + \alpha_U^{(j)}|} \sin \frac{|-\alpha_Q^{(i)} + \alpha_U^{(j)}|}{2} \quad (48)$$

$$M_{ij}^D = \cos \frac{|-\alpha_Q^{(i)} + \alpha_D^{(j)}|}{2} + i \frac{-\alpha_{Qx}^{(i)} + \alpha_{Dx}^{(j)}}{|-\alpha_Q^{(i)} + \alpha_D^{(j)}|} \sin \frac{|-\alpha_Q^{(i)} + \alpha_D^{(j)}|}{2} \quad (49)$$

where $|\alpha| \equiv \sqrt{\alpha_x^2 + \alpha_y^2 + \alpha_z^2}$ and $N = 3$ have been employed.

First, the real and imaginary parts of each mass element are well independent, because once $|-\alpha_Q^{(i)} + \alpha_U^{(j)}|$ is fixed, we still have the freedom to choose $(-\alpha_{Qx}^{(i)} + \alpha_{Ux}^{(j)})/|-\alpha_Q^{(i)} + \alpha_U^{(j)}|$ to be anywhere between -1 and 1 . That is each of M_{ij}^U (and M_{ij}^D) can practically have an arbitrary complex phase. Once we diagonalize the matrices $[M^U M^{U\dagger}]$ and $[M^D M^{D\dagger}]$, those phases will combine and transform themselves into the phases of CKM matrix to give rise to the CP violation processes via the well-known Kobayashi-Maskawa mechanism. Second, we also see that (48), (49) can accommodate a vast class of mass matrix hierarchy. Just to mention some simplest examples, when $\vec{\alpha}_Q^{(i)} = \vec{\alpha}_U^{(j)}$ we obtain a democratic mass matrix (see e.g. [14]), and when $\vec{\alpha}_Q$ and $\vec{\alpha}_U$ point along the x -direction ($|\alpha_Q^{(i)}| = \alpha_{Qx}^{(i)}$, $|\alpha_U^{(j)}| = \alpha_{Ux}^{(j)}$), a pure phase mass matrix [15, 16, 17] for up sector. Numerical analysis on the realization of fermion mass hierarchy via 4D deconstruction is presented in details in a parallel work [12].

IV. CONCLUSION

We have investigated the structure of fermion states in their mass eigenbasis following a pure 4-dimensional deconstruction process. The zero modes expose some interesting localization pattern, that can have useful applications in phenomenology. It is found that the ratio of the two underlying UV breaking scales in the deconstruction scenario is primarily responsible for such localization. The chiral boundary conditions used to obtain chiral zero mode also have crucial influence on the structure of the whole spectrum. CBCs can be put in different classes, each of which characterizes a single mass spectrum. The modification in CBC leads to the change in wave functions and their overlaps in the flavor space. This interactive relation can be used to model the complex CKM mixing of fermion flavors in the Standard Model.

In this paper we have identified the importance of CBC, but have not discussed their

generation mechanism. We hope to come back to this as well as to other related issues concerning gauge boson sector in 4D deconstruction in future work.

Acknowledgments

This work is supported in part by the U.S. Department of Energy under Grant No. DE-A505-89ER40518. N-K.T. also acknowledges the Dissertation Year Fellowship from UVA Graduate School of Arts and Sciences.

APPENDIX A: LATTICIZED EXTRA DIMENSION AND DECONSTRUCTION

We consider in this appendix a simple deconstruction scenario with a product of Abelian groups $\prod_{n=1}^N U(1)_n$. The argument can be generalized to non-Abelian case. The connection of this scenario to a latticized extra dimension is based on the observation that the deconstruction link field and the Wilson line along extra dimension have similar gauge transformation. Therefore we perform the following identification

$$\phi_{n,n+1} \sim e^{ig \int_{na}^{(n+1)a} dy A_5} \quad (\text{A1})$$

where g denotes the gauge coupling, a the lattice spacing, A_5 the extra dimensional component of gauge boson, y the coordinate of extra dimension. The latticization of the fifth dimension also allows us to write $\partial_5 \psi \equiv \partial\psi/\partial y \sim (\psi_{n+1} - \psi_{n-1})/2a$, so that in the gauge $A_5 = 0$ the extra dimensional piece of kinetic term becomes

$$\bar{\psi} \gamma^5 \partial_5 \psi \sim \frac{1}{2a} (\bar{\psi}_n \gamma^5 \phi_{n,n+1} \psi_{n+1} + H.c.) \quad (\text{A2})$$

where the link field has been inserted to assure the gauge invariance. The γ_5 is a remnant of the fifth dimension and leads to a profound difference between latticized ED and pure 4D deconstruction as we will see below. By using (A2), the fermionic mass term of the latticized Lagrangian can be written (apart from a bare mass) in the chiral basis as

$$\sum_{n=1}^N (\bar{\psi}_{nR} \phi_{n,n+1} \psi_{n+1L} - \bar{\psi}_{nL} \phi_{n,n+1} \psi_{n+1R} + H.c.) \quad (\text{A3})$$

We again note that the difference in the sign of these two terms originates from the chiral matrix γ_5 . The mass spectrum induced by (A3) is found to be (see [6])

$$M_n^2 = M^2 + V^2 \sin^2[(2n+1)\pi/N] \quad (\text{A4})$$

where V is the VEV of link fields and M is the bare mass that has not explicitly written in (A3). It is argued in [6] that half of these modes results from a lattice artifact and stands for the fermion flavor doubling problem of lattice gauge theory. To remove the spurious fermionic modes, it is proposed to add the Wilson term $\eta\bar{\psi}(\partial_5 + igA_5)^2\psi/V$ to the 5D Lagrangian, where η is some dimensionless constant. In the result, (A3) now becomes

$$\sum_{n=1}^N \left[(1 - \eta)\bar{\psi}_{nR}\phi_{n,n+1}\psi_{n+1L} - (1 + \eta)\bar{\psi}_{nL}\phi_{n,n+1}\psi_{n+1R} + H.c. \right] \quad (\text{A5})$$

Choosing $\eta = 1$ or -1 one can solve the flavor doubling problem but obviously either choices also eliminate half of fermionic chiral degree of freedom. Therefore in the models inspired by latticized extra dimension, fermions to begin with can be chosen to be Weyl spinors. In the 4D deconstruction approach, however, the whole spectrum of fermions is physical and we retain twice as many chiral modes. That is, fermions to start with are all Dirac spinors.

- [1] N. Arkani-Hamed, A. G. Cohen and H. Georgi, Phys. Rev. Lett. **86**, 4757 (2001).
- [2] C. T. Hill, S. Pokorski and J. Wang, Phys. Rev. D **64**, 105005 (2001).
- [3] W. Skiba and D. Smith, Phys. Rev. D **65**, 095002 (2002).
- [4] H. Abe, T. Kobayashi, N. Maru and K. Yoshioka Phys. Rev. D **67**, 045019 (2003).
- [5] H-C. Cheng, C. T. Hill, S. Pokorski and J. Wang, Phys. Rev. D **64**, 065007 (2001).
- [6] C. T. Hill and A. K. Leibovich, Phys. Rev. D **66**, 016006 (2002).
- [7] F. Bauer, M. Lindner and G. Seidl, J. High Energy Phys. **0405**, 026 (2004).
- [8] H-C. Cheng, C. T. Hill and J. Wang, Phys. Rev. D **64**, 095003 (2001).
- [9] R. Jackiw and S. Rebbi, Phys. Rev. D **13**, 3398 (1976); N. Arkani-Hamed and M. Schmaltz, Phys. Rev. D **61**, 033005 (2000); H. Georgi, A. K. Grant and G. Hailu, Phys. Rev. D **63**, 064027 (2001); P. Q. Hung and N-K. Tran, Phys. Rev. D **69**, 064003 (2004).
- [10] H. Georgi, hep-ph/0408067
- [11] G. H. Golub and C. F. van Loan, *Matrix Computations*, 3th ed. (Johns Hopkins University Press, Baltimore, 1996), W. H. Press, S. A. Teukolosky, W. T. Vetterling and B. P. Flannery, *Numerical Recipes in C*, 2nd ed. (Cambridge University Press, New York, 1992).
- [12] P. Q. Hung, A. Soddu and N-K. Tran, hep-ph/0410179
- [13] S. Nojiri, S. D. Odintsov and A. Sugamoto, Phys. Lett. **B590**, 239 (2004).

- [14] P. Kaus and S. Meshkov, Phys. Rev. D **42**, 1863 (1990).
- [15] G. C. Branco, J. I. Silva-Marcos and M. N. Rebelo, Phys. Lett. B **237**, 446 (1990).
- [16] P. Fishbane and P. Q. Hung, Phys. Rev. D **57**, 2743 (1998).
- [17] P. Q. Hung and M. Seco, Nucl. Phys. B **653**, 123 (2003), P. Q. Hung, M. Seco and A. Soddu, Nucl. Phys. **B692**, 83 (2004).
- [18] C. Csaki, C. Grojean, J. Hubisz, Y Shirman and J. Terning, Phys. Rev. D **70**, 015012 (2004).
- [19] C. Csaki, C. Grojean, L. Pilo and J. Terning, Phys. Rev. Lett **92**, 101802 (2004).
- [20] However, we will still use the ED picture to enhance the visualization effect of physical explanation wherever it is appropriate.
- [21] One can always construct the link field potential and choose its parameters, so that a complex VEV is produced [7]
- [22] Other CBCs can be transformed into (6) by a permutation or an unitary rotation (see Section III).
- [23] As the bare mass M is dynamically generated through the breaking of a gauge-singlet (background) scalar ϕ_S (Eq. (1)), the analogy with the original Jackiw-Rebbi mechanism [9] is clear.
- [24] Any boundary condition can be written in a gauge-invariant form by incorporating an appropriate product of link fields, e.g. CBC $\frac{\phi_{k,k+1}}{V} \dots \frac{\phi_{q-1,q}}{V} \psi_{qL} = \psi_{kL}$ is gauge-invariant and implies a simple relation $\psi_{qL} = \psi_{kL}$ after the spontaneous symmetry breaking $\langle \phi \rangle = V$
- [25] The rotation is completely characterized by the CBC on the corresponding quark, as shown in Section IIIB.
- [26] Within the three-site gauge model $[SU(2) \times U(1)]^3$ under consideration, there is no interaction that can violate the baryon number. Moreover, even if a larger GUT scenario is incorporated at some higher energy scale, one can always choose appropriate CBCs and parameter ρ for lepton sector to produce a sufficiently small quark-lepton mixing interaction. Since a more quantitative treatment of lepton sector lies beyond the scope of this paper, here we will not pursue further the issues of baryogenesis and proton decay.